(LCR), as well as comprehensive physical insight. A comparison with L-band experimental data has shown very good agreement. This new method is believed to be a useful complement to system designers in the fields of fade mitigation techniques and diversity signal processing.

© IEE 2001 *17 April 2001*
Electronics Letters Online No: 20010550
DOI: 10.1049/el:20010550

C. Oestges (*Information Systems Laboratory, Stanford University, Packard Building, 350 Serra Mall, Stanford, CA 94305, USA*)

D. Vanhoenacker-Janvier (*Microwave Laboratory, Université catholique de Louvain, Maxwell Building, 3 place du Levant, 1348 Louvain-la-Neuve, Belgium*)

C. Oestges: On leave from the Microwave Laboratory, Université catholique de Louvain, Belgium)

References

1 KANATAS, A.G., KOUNTOURIS, I.D., KOSTARAS, G.B., and CONSTANTINOU, P.: 'A UTD propagation model in urban microcellular environments', *IEEE Trans. Veh. Technol.*, 1997, **46**, (1), pp. 185–193
2 KOUYOUMJIAN, R.G., and PATHAK, P.H.: 'A uniform geometrical theory of diffraction for an edge in a perfectly conducting surface', *Proc. IEEE*, 1974, **62**, (11), pp. 1448–1461
3 MICHAELI, A.: 'Equivalent currents for arbitrary aspects of observation', *IEEE Trans. Antennas Propag.*, 1984, **32**, (3), pp. 252–258
4 OESTGES, C.: 'Propagation modelling of low-earth orbit satellite personal communication systems'. PhD thesis, Université catholique de Louvain, 2000
5 BALANIS, C.A.: 'Antenna theory: analysis and design' (Harper & Row, New York, 1982)
6 KNOTT, E.F., and SENIOR, T.B.A.: 'Comparison of three high-frequency diffraction techniques', *Proc. IEEE*, 1974, **62**, (11), pp. 1468–1474
7 KANATAS, A.G., and CONSTANTINOU, P.: 'City center high-elevation angle propagation measurements at L band for land mobile-satellite systems', *IEEE Trans. Veh. Technol.*, 1998, **47**, (3), pp. 1002–1011
8 OESTGES, C., and VANHOENACKER-JANVIER, D.: 'Experimental validation and system applications of ray-tracing model in built-up areas', *Electron. Lett.*, 2000, **36**, (5), pp. 461–462

0.25 μm gate-length, MBE-grown AlGaN/GaN HEMTs with high current and high f_T

V. Kumar, W. Lu, R. Schwindt, J. Van Hove, P. Chow and I. Adesida

MBE-grown AlGaN/GaN high electron mobility transistors (HEMTs) on sapphire substrates have been fabricated. These 0.25 μm gate-length devices exhibited a maximum drain current density as high as 1.39 A/mm, a unity gain cutoff frequency (f_T) of 67 GHz, and a maximum frequency of oscillation (f_{max}) of 136 GHz. The f_T of 67 GHz and f_{max} of 136 GHz are the highest reported values for 0.25 μm gate-length GaN-based HEMTs.

GaN-based high electron mobility transistors (HEMTs) are promising devices for high power and high temperature applications [1 – 3]. This potential is due to advantageous material properties such as a wide bandgap leading to high breakdown voltage, a high saturated-electron drift velocity and the existence of AlGaN/GaN heterostructures with a high conduction band offset and high piezoelectricity resulting in high sheet carrier densities in the 10^{13} cm^{-2} range. Recently, tremendous progress has been recorded in the material quality and device processing of GaN-based HEMTs. This has resulted in significant improvement in the DC and RF performances of these devices. AlGaN/GaN HEMTs with a current density as high as 1.7 A/mm have been reported [4]. 50 nm gate-length AlGaN/GaN HEMTs with a record unity gain cutoff frequency (f_T) 110 GHz and maximum frequency of oscillation (f_{max}) over 140 GHz have been demonstrated [5].

In this Letter, we report the simultaneous achievement of the high current density and high cutoff frequencies for 0.25 μm gate-length AlGaN/GaN HEMTs on sapphire substrates grown by molecular beam epitaxy (MBE). The current density of 1.39 A/mm, f_T of 67 GHz and f_{max} of 136 GHz represent significant improvements for AlGaN/GaN HEMTs of similar gate-lengths on sapphire substrates.

The layer used here was grown on sapphire substrates by molecular beam epitaxy (MBE). The epilayer consists of 2 μm undoped GaN, 30 nm undoped $Al_{0.24}Ga_{0.76}N$ and a 5 nm undoped GaN cap layer. Hall measurements showed a sheet carrier concentration of 1.5×10^{13} cm^{-2} and an electron mobility of 1170 cm^2/Vs. Device fabrication started with mesa isolation using Cl_2 plasma in an inductively-coupled-plasma reactive ion etch (ICP-RIE) system. Ohmic contacts were formed by rapid thermal annealing of evaporated Ti/Al/Ti/Au at 860°C for 30 s. Using on-wafer transfer length measurement (TLM) patterns, the ohmic contact resistance was typically measured to be ~0.35 Ωmm. Mushroom-shaped gates (Ni/Au) with gate-length (L_g) of 0.25 μm were fabricated using electron-beam lithography. The devices had a gate width of 100 μm and a source drain spacing of 2 μm.

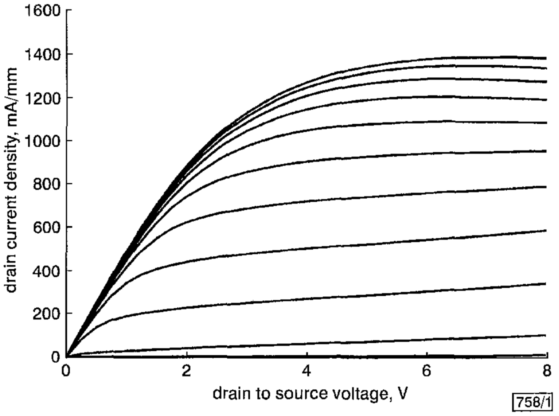

Fig. 1 *DC I_D-V_{DS} characteristics of 0.25 × 100 μm AlGaN/GaN HEMT on sapphire substrate*

Gate bias was swept from 2 to –8 V in steps of –1 V

The DC measurements were carried out using an HP4145B semiconductor parameter analyser. Fig. 1 shows the typical drain current-voltage (I_D-V_{DS}) characteristics of a device. The gate was biased from 2 to –8 V in steps of –1 V. The devices exhibited a maximum drain current density of 1.39 A/mm at a gate bias of 2 V and a drain bias of 7 V. To our knowledge this is the highest value ever reported for GaN-based HEMTs on a sapphire substrate. The DC transfer characteristics are shown in Fig. 2. The drain was biased at 5 V. A peak extrinsic transconductance (g_m) of 216 mS/mm was measured at $V_{gs} = -6.6$ V and $V_{ds} = 5$ V.

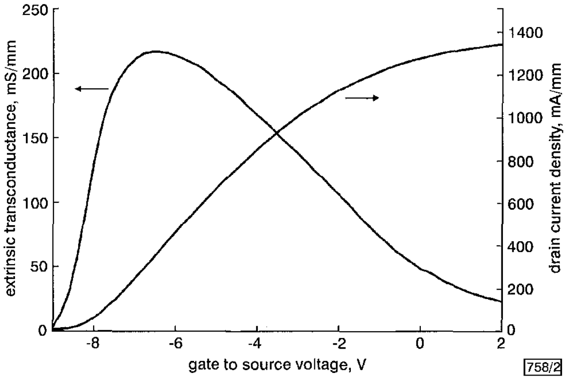

Fig. 2 *DC transfer characteristics of 0.25 × 100 μm AlGaN/GaN HEMT on sapphire substrate*

Drain bias was 5 V

RF measurements were carried out on-wafer using an HP8510C network analyser in the 1 to 50 GHz range. Fig. 3 shows the short-circuit current gain ($|h_{21}|$) and maximum available power gain (G_{Amax}) derived from on-wafer S-parameters measurements against frequency. The values of unity gain cutoff frequency (f_T) and maximum frequency of oscillation (f_{max}) were determined by extrapolation of the $|h_{21}|$ and G_{Amax} data at −20 dB/decade. At a drain bias of 10 V and a gate bias of −6.7 V, an f_T of 67 GHz and f_{max} of 136 GHz were obtained, which to the best of the authors' knowledge are again the highest data ever reported for 0.25 µm gate-length GaN-based FETs.

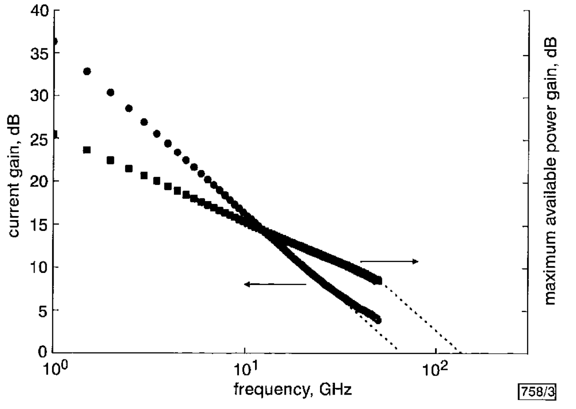

Fig. 3 *Short-circuit current gain* ($|h_{21}|$) *and maximum available power gain* (G_{Amax}) *of typical 0.25 × 100 µm AlGaN/GaN HEMT on sapphire substrate*

Device was biased at V_{DS} = 10 V and V_{GS} = −6.7 V

In summary, we have presented 0.25 µm gate-length, MBE-grown high current density (1.39 A/mm) AlGaN/GaN HEMTs on sapphire substrates. The measured values of f_T of 67 GHz and f_{max} of 136 GHz are the highest reported data for 0.25 µm gate-length GaN-based HEMTs.

Acknowledgments: This work was supported at UIUC by a grant from Triquint Corporation and Air Force Grant 92768C2TOS through TRW Corporation.

27 March 2001

Electronics Letters Online No: 20010582

DOI: 10.1049/el:20010582

V. Kumar, W. Lu, R. Schwindt and I. Adesida (*Department of Electrical and Computer Engineering, Microelectronics Laboratory, University of Illinois at Urbana-Champaign, Urbana, IL-61801, USA*)

J. Van Hove and P. Chow (*SVT Associates, 7620 Executive Drive, Eden Prairie, MN-55344, USA*)

References

1 WU, Y.F., KAPOLNEK, D., IBBETSON, J., ZHANG, N.Q., PARIKH, P., KELLER, B.P., and MISHRA, U.K.: 'High Al-content AlGaN/GaN HEMTs on SiC substrates with very-high performance'. IEDM Tech. Dig., 6-8 Dec. 1999, pp. 927–929

2 SHEPPARD, S.T., DOVERSPIKE, K., PRIBBLE, W.L., ALLEN, S.T., and PALMOUR, J.W.: 'High power microwave GaN/AlGaN HEMTs on silicon carbide', *IEEE Electron Device Lett.*, 1999, **20**, pp. 161–163

3 NGUYEN, N.X., MICOVIC, M., WONG, W.S., HASHIMOTO, P., MCCRAY, L.M., JANKE, P., and NGUYEN, C.: 'High performance microwave power GaN/AlGaN MODFETs grown by RF-assisted MBE', *Electron Lett.*, 2000, **36**, (5), pp. 468–469

4 CHEN, Q., YANG, J.W., KAHN, M.A., PING, A.T., and ADESIDA, I.: 'High transconductance AlGaN/GaN heterostructure field effect transistors on SiC substrates', *Electron Lett.*, 1997, **33**, (16), pp. 1413–1414

5 MICOVIC, M., NGUYEN, N.X., JANKE, P., WONG, W.S., HASHIMOTO, P., MCCRAY, L.M., and NGUYEN, C.: 'GaN/AlGaN high electron mobility transistors with f_T of 110 GHz', *Electron Lett.*, 2000, **36**, (4), pp. 358–359

Measurement of starting torque in surface tension self-assembly of microstructures

R.R.A. Syms

The torque available at the start of out-of-plane rotation in surface tension powered self-assembly of microstructures is measured by deformation of an elastic spring. Values confirm to theoretical estimates and show that surface tension torque can overwhelm the gravitational counter-torque for realistic components in the microstructure size regime.

Surface tension powered self-assembly is a method of constructing three-dimensional microstructures [1, 2]. Movable parts are fabricated flat by surface patterning and sacrificial etching, and rotated out of the wafer plane by a surface tension torque obtained by heating small pads of meltable material linking moving parts to the substrate. The technique has been demonstrated using metal (Pb : Sn solder) [3 – 6], glass (BPSG) [7] and polymer (thick photoresist) [8] as the meltable material, and single-crystal silicon [3, 7], bonded silicon [8], polysilicon [4] and electroplated Ni [3] and Cu [6] as the mechanical material.

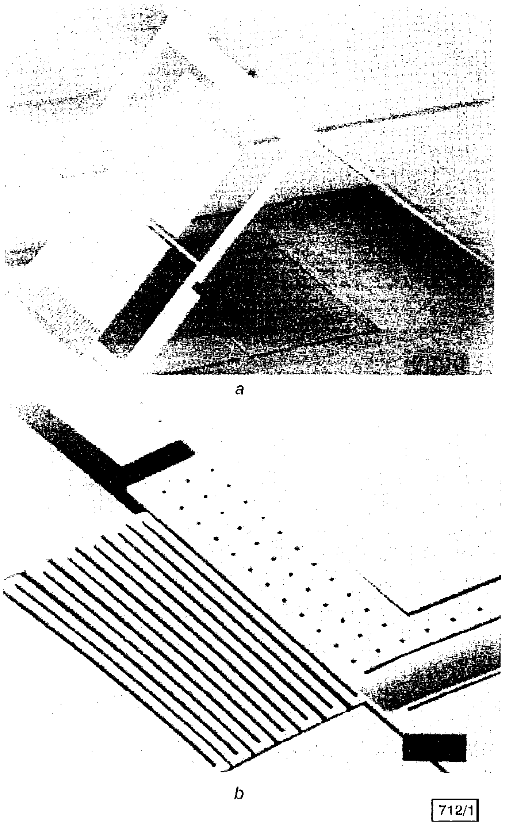

Fig. 1 *Self-assembled 3D optical torsion mirror scanner and torque gauge*

a Torsion mirror scanner
b Torque gauge

Surprisingly large structures (e.g. the torsion mirror scanner shown in Fig. 1*a*, whose frame has a height of 500 µm) can be assembled in this way. Physical considerations suggest that because of its advantageous size scaling, surface tension force (which scales as dimension) should overcome elastic forces (dimension squared) and self-weight (dimension cubed) if the size of a structure is sufficiently reduced. To identify the limits of surface tension self-assembly, it is important to measure the torque available. This can be done with an elastic torque gauge, as we now show.

Fig. 2 shows the geometry, which consists of two self-assembling parts on a 1 mm baseline. Normally, the surface tension torque would cause these to rotate in opposite directions through 45°, until a mechanism is engaged to prevent further movement